

## Interaction of tunnel-coupled quantum dots in a magnetic field

D. S. Duncan, M. A. Topinka, and R. M. Westervelt

*Division of Engineering and Applied Sciences and Department of Physics, Harvard University, Cambridge, Massachusetts 02138*

K. D. Maranowski and A. C. Gossard

*Materials Department, University of California, Santa Barbara, Santa Barbara, California 93106*

(Received 5 July 2000; published 8 January 2001)

An artificial molecule formed by two tunnel-coupled quantum dots in a GaAs/Al<sub>x</sub>Ga<sub>1-x</sub>As heterostructure is studied in perpendicular magnetic fields. Coulomb blockade spectroscopy at low temperatures determines how the binding energy of the artificial molecule evolves with magnetic field. The binding energy and the double-dot ground-state energy exhibit mesoscopic fluctuations due to the coupling of electron wave functions on the individual dots.

DOI: 10.1103/PhysRevB.63.045311

PACS number(s): 73.23.Ad

Two semiconductor quantum dots, known as artificial atoms, can be tunnel coupled together to form an artificial molecule. The tunnel coupling, provided by a quantum point contact, can be varied to change the strength of the molecular bonding. Recent experiments used Coulomb blockade spectroscopy to study the transition from weakly coupled to strongly interacting dots in zero magnetic field<sup>1-4</sup> and in the quantum Hall regime.<sup>5,6</sup> Many interesting effects have been observed in these systems.<sup>7-11</sup> In zero magnetic field, the electrons on two dots were demonstrated to be shared on one large dot<sup>4</sup> at an interdot tunnel coupling  $G_{\text{int}} = 2e^2/h$ , as predicted by theory.<sup>12,13</sup> In the quantum Hall regime, for which transport occurs along edge states in each dot, this transition was found to be complete at  $G_{\text{int}} = e^2/h$ , the value at which the outermost spin-polarized edge states of the two dots join.<sup>5</sup> The binding of artificial molecules has not been studied previously in the weak magnetic-field regime, the subject of this paper.

Understanding the interaction of electron charges and spins in tunnel-coupled quantum dots in magnetic fields is important for fundamental physics and for proposed applications. Multiple quantum dot devices have been proposed as the building blocks of single-electron device circuits<sup>14</sup> as well as for the elements of quantum computers.<sup>15-17</sup> One proposal<sup>15</sup> for a quantum computer qubit is based on interacting electron spins in two tunnel-coupled quantum dots; a magnetic field is used to carry out logic operations. Because the field of experimental quantum computing is just beginning, understanding how electron charges and spins are shared between tunnel-coupled quantum dots in magnetic fields could provide a basis for future quantum computer implementations.

In this paper electron states in tunnel-coupled double-dot artificial molecules are investigated using Coulomb blockade spectroscopy. In contrast to previous work, these experiments study the coupled-dot system in relatively weak magnetic fields ranging from  $B = 0$  T to  $B = 400$  mT, with filling factors  $\nu \geq 31$ . The magnetic field in this regime causes mesoscopic fluctuations in the wave functions and energy levels of electrons in individual dots and hence changes the ground-state energy and molecular binding energy of the artificial molecule. Such fluctuations are ubiquitous in mesoscopic

systems, but they have not been studied previously in a double quantum dot. The magnetic-field dependence of the binding energy is studied over the full range of interdot conductance  $G_{\text{int}}$  from  $G_{\text{int}} \approx 0$  to  $G_{\text{int}} = 2e^2/h \equiv G_Q$ , the conductance quantum for a spin degenerate channel.

Figure 1(a) is a scanning electron microscope photograph of the artificial molecule device, consisting of two quantum dots in series defined in a GaAs/Al<sub>x</sub>Ga<sub>1-x</sub>As heterostructure electrostatically by metal gates fabricated on the surface using electron-beam lithography and Cr-Au metallization. The heterostructure contains a two-dimensional electron gas (2DEG) located 57 nm beneath the surface with mobility

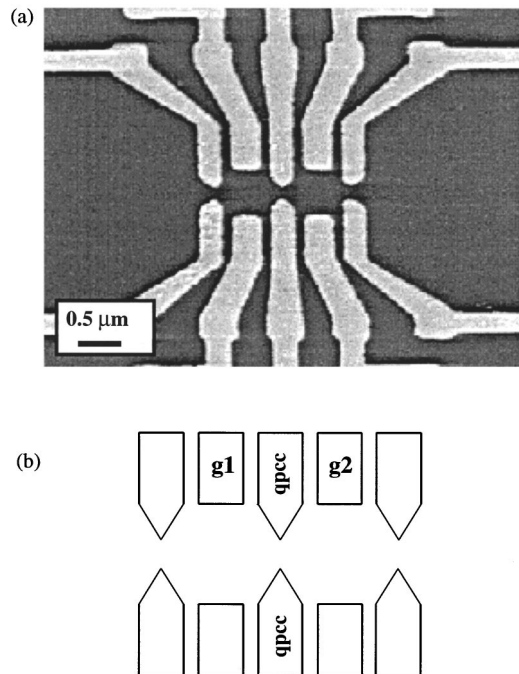


FIG. 1. (a) Scanned electron microscope photograph and (b) schematic diagram of the artificial molecule device, consisting of two quantum dots coupled by a quantum point contact. The conductance of the center quantum point contact determines interdot coupling. Charge can be separately induced on each dot by varying the gate voltages  $V_{g1}$  and  $V_{g2}$ .

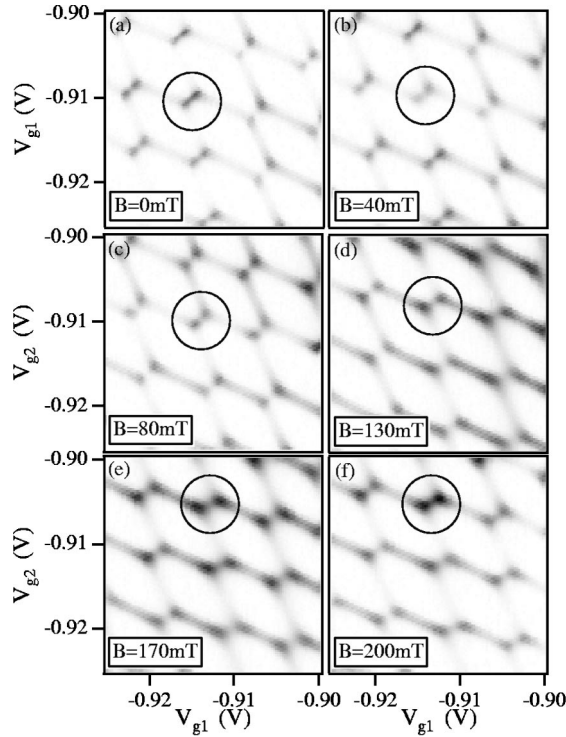


FIG. 2. Coulomb blockade conductance peaks of a tunnel-coupled double quantum dot for increasing perpendicular magnetic field  $B$ . The gray scale images show differential conductance through the double dot vs side gate voltages  $V_{g1}$  and  $V_{g2}$  in perpendicular magnetic fields: (a) 0 mT, (b) 40 mT, (c) 80 mT, (d) 130 mT, (e) 170 mT, and (f) 200 mT. Varying the magnetic field causes reproducible variations in both the peak heights and the peak splitting.

450 000  $\text{cm}^2/\text{Vs}$  and sheet density  $3 \times 10^{11}/\text{cm}^2$ . Each dot has lithographic size  $500 \times 500 \text{ nm}^2$  and contains  $\approx 270$  electrons, assuming a depletion length of 100 nm from the gates. The level spacing in each dot is  $\Delta \epsilon \approx 80 \mu\text{eV}$ . Figure 1(b) is a schematic diagram of the gates. Each dot has two quantum point contacts and two confining side gates; the dots share one point contact, labeled qpcc. The point contact conductances can be individually tuned; the conductance of qpcc determines the interdot coupling. The conductances of the outer point contacts were tuned to the weak tunneling regime. Four side gates define the sides of the quantum dots. The voltages  $V_{g1}$  and  $V_{g2}$  on the side gates labeled  $g_1$  and  $g_2$  are varied to induce charge on the corresponding dot. The differential conductance through the entire series double dot was measured as  $V_{g1}, V_{g2}$ , and a magnetic field  $B$  applied perpendicular to the plane of the sample were varied. The applied drain to source voltage was  $10 \mu\text{V}$ . All measurements were done in a dilution refrigerator at a base temperature of 25 mK.

Figure 2(a) shows a characteristic image of the Coulomb blockade for a tunnel-coupled double dot which can be used to measure the binding energy of the artificial molecule. Figure 2(a) is an inverted gray-scale image of the differential conductance through the series double dot as a function of the voltages  $V_{g1}$  and  $V_{g2}$ . Dark regions are high conductance, light regions are low conductance. The signal consists

of a grid of split conductance peaks, as observed in previous experiments.<sup>4</sup> For weak interdot coupling, peaks in the conductance landscape occur where the Coulomb blockade is simultaneously lifted in both dots. Finite interdot tunneling causes these peaks to split and separate into pairs<sup>13</sup> as shown in Fig. 2(a); the separation is proportional to the lowering of the ground-state energy of the double dot by interdot tunneling, i.e., to the molecular binding energy. The capacitive contribution to the peak separation has been shown to be weak relative to the contribution due to interdot tunneling.<sup>4</sup>

Figures 2(a) to 2(f) illustrate how a perpendicular magnetic field  $B$  introduces mesoscopic fluctuations in the binding energy of the artificial molecule and the Coulomb blockade peak intensity. The images in Fig. 2 were taken for increasing magnetic fields: (a) 0 mT, (b) 40 mT, (c) 80 mT, (d) 130 mT, (e) 170 mT, and (f) 200 mT. The interdot conductance is set at  $G_{\text{int}} = 0.8G_Q$  for these measurements. As in Fig. 2(a) the  $x$  and  $y$  axes are the side gate voltages  $V_{g1}$  and  $V_{g2}$  and the intensity shows the differential conductance through the double dot. In each image in Fig. 2 an array of split conductance peaks is observed. The magnetic field changes both the measured peak splitting and the measured peak heights. The changes are not monotonic, but fluctuate in both directions as the magnetic field is increased; this can be seen by following a single split peak throughout the series. Not all of the peak doublets shown fluctuate in exactly the same manner, though there is some correlation in the behavior of neighboring peak doublets. These changes are exactly reproducible as the field is ramped up and down. Large shifts in position of the charging pattern were caused by switching noise in the sample, observed in scans at intermediate magnetic fields.

Changes in the double-dot Coulomb blockade peak splitting and intensity with magnetic field are illustrated more dramatically in Fig. 3(b). The data were taken by connecting gates  $g_1$  and  $g_2$  together, making a diagonal cut through the two-dimensional gate voltage landscape. The dots were tuned via the side gates opposite gates  $g_1$  and  $g_2$  so that varying the voltage  $V_{g1} = V_{g2}$  would cut precisely through the center of a series of conductance peak doublets at  $B = 0$ . The desired path is indicated by the dashed line in Fig. 3(a), taken before this tuning. In Fig. 3(b) the Coulomb blockade peak splitting and intensity are plotted vs magnetic field  $B$ . As the magnetic field is increased above  $B = 0$  T, nonmonotonic changes in both peak splitting and peak intensity are observed. The variations are almost perfectly symmetric about  $B = 0$  T; deviations from symmetry are expected due to switching noise. Observing this symmetry about  $B = 0$  T provides a confirmation that the fluctuations are primarily caused by the magnetic field. The evolution of three consecutive peak pairs is observed in this diagram, and all three evolve in a similar fashion with the magnetic field.

The data of Fig. 3(b) can be explained qualitatively by considering the interplay of a number of effects the magnetic field has on the double-dot system. First, the magnetic field changes classical electron trajectories within the dots as well as the spatial distribution of electron wave functions. The Coulomb blockade peak heights depend on the degree of overlap of the electron wave functions in each dot and its

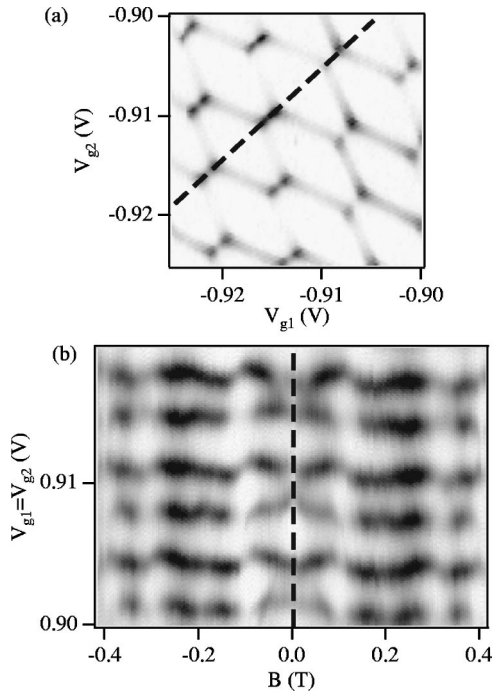


FIG. 3. Measured fluctuations in the Coulomb blockade peak splitting and intensity of tunnel-coupled double dot with magnetic field: (a) Array of split peaks; dashed line indicates a diagonal cut through the conductance peaks. (b) Differential conductance through the double dot vs magnetic field  $B$  and gate voltage  $V_{g1} = V_{g2}$ . The gate voltage path was positioned along the dashed line in (a) at  $B = 0$  T, by tuning the side gates opposite gates  $g1$  and  $g2$  before the magnetic-field sweep. Strong, reproducible fluctuations in the peak splitting and in the peak height are observed with increasing magnetic field; these variations are symmetric about  $B = 0$  T.

lead. As the magnetic field is varied the overlaps change and consequently the heights of the conductance peaks change. Second, changing the spatial distribution of electron wave functions changes the overlap of wave functions on different dots and the interdot tunneling matrix elements. As a result, the interdot coupling, ground-state energy, and molecular binding energy change, as seen by changes in peak splitting in Fig. 3(b). Finally, changing the magnetic field causes shifts in the single-electron states in the individual dots, manifested as shifts in the positions of the peak doublets in the two-dimensional conductance landscape in Fig. 3(a). The resulting shifts in peak-doublet position can be sufficient to cause the diagonal line  $V_{g1} = V_{g2}$  along which the measurement is made to cut through the two-dimensional 2D gate-voltage landscape off the side of the peak doublet, resulting in a decrease in the measured peak heights, as seen in Fig. 3(b).

Mesoscopic fluctuations in artificial molecules were addressed by recent theory<sup>18</sup> predicting fluctuations in double-dot properties which depend on the interdot tunnel coupling. In previous theoretical work,<sup>13</sup> the interdot tunneling matrix elements were assumed to be constant for the range of levels of interest. In reality, these matrix elements have a statistical distribution and cause apparently random fluctuations in the

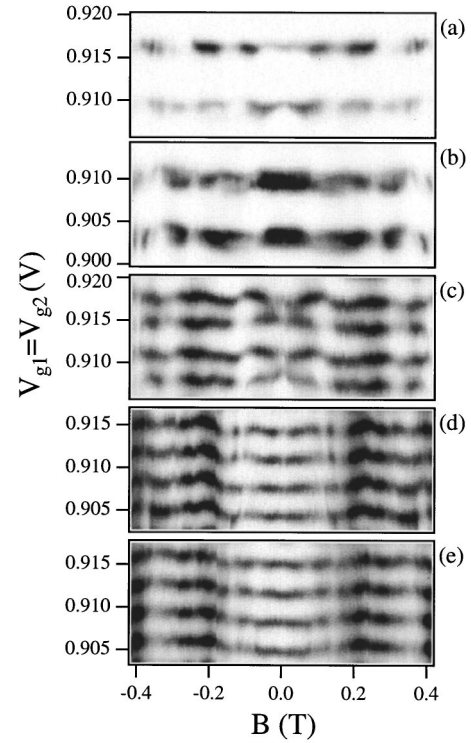


FIG. 4. Effect of interdot tunnel conductance  $G_{\text{int}}$  on the Coulomb blockade peak splitting and intensity with  $V_{g1} = V_{g2}$ , positioned to pass through the conductance peaks at  $B = 0$  by tuning the side gates opposite gates  $g1$  and  $g2$  before the magnetic-field sweep, for interdot conductance values of (a)  $0.5G_Q$ , (b)  $0.86G_Q$ , (c)  $1.5G_Q$ , (d)  $1.98G_Q$ , and (e)  $2.3G_Q$ , with  $G_Q = 2e^2/h$ . As the interdot coupling is increased, the peaks split from single peaks in (a) to twice the number of peaks with half the spacing in (d), as predicted by theory for the case where  $G_{\text{int}} = G_Q$ .

double-dot properties. These mesoscopic fluctuations were studied theoretically assuming a spatial distribution of electron wave functions derived from random matrix theory.<sup>18</sup> Such fluctuations have been characterized in single quantum dots<sup>19–21</sup> but have not been explicitly studied in double quantum dots due to the difficulty of obtaining statistics in double-dot measurement setups. Such fluctuations are clearly seen in our magnetic-field data, although the data are not sufficient in quantity to make quantitative comparison with the statistical distributions predicted by theory.

Figure 4 shows how mesoscopic fluctuations of the Coulomb blockade peak splitting and peak intensity depend on the interdot conductance  $G_{\text{int}}$ . Figures 4(a) through 4(e) show the differential conductance through the double dot plotted in inverse gray scale vs the magnetic field  $B$  and the gate voltage  $V_{g1} = V_{g2}$ . The dots were tuned via the side gates opposite gates  $g1$  and  $g2$  so that varying the voltage  $V_{g1} = V_{g2}$  would cut precisely through the center of a series of conductance peak doublets at  $B = 0$ . Each of the five graphs was taken at a different value of  $G_{\text{int}}$ : (a)  $0.5G_Q$ , (b)  $0.87G_Q$ , (c)  $1.5G_Q$ , (d)  $1.98G_Q$ , and (e)  $2.3G_Q$ . In Fig. 4(a) the interdot conductance is weak and no peak splitting is observable. However, the magnetic field still causes large variations in the peak heights, and the regions in which the

peak heights drop dramatically extend over longer ranges of  $B$  than in Fig. 3(b). This is further evidence that shifts in the discrete energy levels cause these large fluctuations: at lower values of  $G_{\text{int}}$  the widths of the peak doublets are narrower, and small shifts in their positions cause more dramatic effects. As the interdot coupling is increased in Fig. 3(b), the peak widths appear to broaden in the vertical direction, due to an increase in peak splitting that is not resolvable. As the interdot coupling is increased in Fig. 3(c), the split peaks become resolvable and the fluctuations in position become more striking. At a value of  $G_{\text{int}} = G_Q$  in Fig. 4(d), the period of the peaks in the vertical direction has doubled, indicating the two dots have merged into one large dot with twice the area. This behavior is maintained as the interdot coupling is

increased further in Fig. 4(e), as predicted by theory for the case of  $B = 0$  T. This is in contrast to the quantum Hall regime behavior<sup>5</sup> where the two dots join completely at  $G_{\text{int}} = e^2/h$ , due to the removal of spin degeneracy by the large magnetic field.

We thank C.M. Marcus and P.W. Brouwer for valuable discussions. This work was supported at Harvard by ONR Grant No. N00014-99-1-0347, ONR/AASERT Grant No. N00014-97-1-0770, ONR Grant No. N00014-95-1-0104, NSF Grant No. NSF DMR-98-0-2242, and the MRSEC program of the NSF under Grant No. DMR-98-09363, and at UCSB by QUEST, a NSF Science and Technology Center.

- 
- <sup>1</sup>F. R. Waugh, M. J. Berry, C. H. Crouch, C. Livermore, D. J. Mar, R. M. Westervelt, K. L. Campman, and A. C. Gossard, *Phys. Rev. B* **53**, 1413 (1996).
- <sup>2</sup>F. R. Waugh, M. J. Berry, D. J. Mar, R. M. Westervelt, K. L. Campman, and A. C. Gossard, *Phys. Rev. Lett.* **75**, 705 (1995).
- <sup>3</sup>C. H. Crouch, C. Livermore, R. M. Westervelt, K. L. Campman, and A. C. Gossard, *Appl. Phys. Lett.* **71**, 817 (1997).
- <sup>4</sup>C. Livermore, C. H. Crouch, R. M. Westervelt, K. L. Campman, and A. C. Gossard, *Science* **274**, 1332 (1996).
- <sup>5</sup>C. Livermore, D. S. Duncan, R. M. Westervelt, K. D. Maranowski, and A. C. Gossard, *J. Appl. Phys.* **86**, 4043 (1999).
- <sup>6</sup>C. Livermore, D. S. Duncan, R. M. Westervelt, K. D. Maranowski, and A. C. Gossard, *Phys. Rev. B* **59**, 10 744 (1999).
- <sup>7</sup>N. C. van der Vaart, S. F. Godijn, Y. V. Nazarov, C. J. P. M. Harmans, J. E. Mooij, L. W. Molenkamp, and C. T. Foxon, *Phys. Rev. Lett.* **74**, 4702 (1995).
- <sup>8</sup>R. H. Blick, R. J. Haug, J. Weis, D. Pfannkuche, K. V. von Klitzing, and K. Eberl, *Phys. Rev. B* **53**, 7899 (1996).
- <sup>9</sup>R. H. Blick, D. W. van der Weide, R. J. Haug, and K. Eberl, *Phys. Rev. Lett.* **81**, 689 (1998).
- <sup>10</sup>D. Dixon, L. P. Kouwenhoven, P. L. McEuen, Y. Nagamune, J. Motohisa, and H. Sakaki, *Phys. Rev. B* **53**, 12 625 (1996).
- <sup>11</sup>T. H. Oosterkamp, T. Fujisawa, W. G. van der Wiel, K. Ishibashi, R. V. Hijman, S. Tarucha, and L. P. Kouwenhoven, *Nature (London)* **395**, 873 (1998).
- <sup>12</sup>K. A. Matveev, *Phys. Rev. B* **51**, 1743 (1995).
- <sup>13</sup>J. M. Golden and B. I. Halperin, *Phys. Rev. B* **53**, 3893 (1996).
- <sup>14</sup>*Single Charge Tunneling*, edited by H. Grabert and M. H. Devoret, NATO Advanced Study Institute Series B: Physics, Vol. 294 (Plenum, New York, 1992).
- <sup>15</sup>G. Burkard, D. Loss, and D. P. DiVincenzo, *Phys. Rev. B* **59**, 2070 (1999).
- <sup>16</sup>D. Loss and D. P. DiVincenzo, *Phys. Rev. A* **57**, 120 (1999).
- <sup>17</sup>D. Loss and E. V. Sukhorukov, *Phys. Rev. Lett.* **84**, 1035 (2000).
- <sup>18</sup>A. Kaminski and L. I. Glazman, *Phys. Rev. B* **59**, 9798 (1999).
- <sup>19</sup>J. A. Folk, S. R. Patel, S. F. Godijn, A. G. Huibers, S. M. Cronenwett, C. M. Marcus, K. Campman, and A. C. Gossard, *Phys. Rev. Lett.* **76**, 1699 (1996).
- <sup>20</sup>S. M. Cronenwett, S. R. Patel, C. M. Marcus, K. Campman, and A. C. Gossard, *Phys. Rev. Lett.* **79**, 2312 (1997).
- <sup>21</sup>S. M. Maurer, S. R. Patel, C. M. Marcus, C. I. Duruoz, and J. S. Harris, *Phys. Rev. Lett.* **83**, 1403 (1999).